Friction **11**(7): 1165–1176 (2023)
https://doi.org/10.1007/s40544-022-0640-7
ISSN 2223-7690
CN 10-1237/TH

RESEARCH ARTICLE

Insight into the high-temperature tribological mechanism of VAlTiCrW high entropy alloy film: AlV_3O_9 from tribochemistry

Xuesong LIU[1,2], Jun FAN[2], Jibin PU[2,*], Zhaoxia LU[1,*]

[1] *College of Chemistry and Chemical Engineering, Guangxi University, Nanning 530004, China*

[2] *Key Laboratory of Marine Materials and Related Technologies, Key Laboratory of Marine Materials and Protective Technologies of Zhejiang Province, Ningbo Institute of Materials Technology and Engineering, Chinese Academy of Sciences, Ningbo 315201, China*

Received: 11 February 2022 / Revised: 21 March 2022 / Accepted: 21 April 2022

Abstract: High-entropy alloys have made significant progress in high mechanical properties, wear resistance, and corrosion resistance properties. Excellent tribological properties, especially high-temperature lubrication, have become another sought performance. In this work, VAlTiCrW high-entropy alloy film with body-centered cubic (BCC) structure was prepared on superalloy substrate by magnetron sputtering. It is found that the VAlTiCrW film shows very low friction coefficient of 0.15 and a low wear rate of 10^{-5} orders of magnitude at 800 °C. After 800 °C oxidation, the film can still obtain a friction coefficient of no more than 0.2 at 700 °C. XRD and TEM revealed the formation of ternary oxide AlV_3O_9 with preferred orientation of (002) crystal plane with large spacing of 0.71 nm on the wear surface of the film, a high-temperature lubricating phase that has not been reported, realizes the low friction coefficient. This AlV_3O_9 can be formed by tribochemical reaction under the thermal-mechanical action at 700 °C, but pre-oxidation at 800 °C is the prerequisite in order to form the precursors of V-rich and Al-rich oxide layer.

Keywords: high entropy alloy; high temperature friction; AlV_3O_9; oxide

1 Introduction

The high coefficient of friction of power components operating at high temperatures (e.g., bearings and gears in aero engines) can lead to increased wear. When the friction coefficient of power components working at high temperature exceeds 0.2, it will lead to irreversible deformation of contact surface, which will reduce the reliability and shorten the service life of components [1–3]. Improving the surface tribological properties of components by solid lubricating materials is an effective way to protect components [4]. Commonly used solid lubricating materials, such as disulfide and carbon coatings, can only exert lubricating effects below 300 °C. Current research has shown that solid lubricating materials for medium and high temperature applications can be broadly classified into three categories: soft metals, fluorides [5], and metal oxides [1, 6]. However, soft metals (such as lead and silver) will eventually oxidize to oxides at high temperatures, while fluoride (barium fluoride and calcium fluoride) inevitably causes environmental pollution [7]. Metal oxides have high rigidity and thermal stability. Currently, there are not only binary oxides (such as V_2O_5, WO_3, ReO_3, etc.), but also ternary oxides (such as $PbMoO_4$ [8], $ZnWO_4$ [9], Ag_3VO_4 [10], $AgNbO_3$ [11]), which are effective lubricants in high temperature environment.

Oxidation of materials is inevitable at high temperatures, so the tribological characteristics of the oxide layer dominate the friction and wear properties of the materials at high temperatures [12]. According to the lubricating properties of oxides, when the coating contains metals with high ionic potential such as Re,

* Corresponding authors: Jibin PU, E-mail: pujibin@nimte.ac.cn; Zhaoxia LU, E-mail: zhaoxialu@gxu.edu.cn

B, V, Mo, and W, it is favorable to form oxides with oxygen vacancies. Owing to the existence of these oxygen vacancies, the oxides are easily sheared which helps to reduce the friction coefficient [13–15]. Therefore, *in-situ* oxidation of the alloy with designed composition to obtain a lubricating glaze layer is an effective method to reduce the friction coefficient and wear rate at high temperatures.

High-entropy alloy films usually composed of five or more multi-principal elements provide a new way of thinking for friction reduction in high-temperature environments. Multi-principal elements facilitate the design of structure and properties. By optimizing mixing entropy, mixing enthalpy, atomic size difference, and valence electron concentration, the high-entropy alloy film can exhibit a single body-centered cubic (BCC), face-centered cubic (FCC), or hexagonal dense structure (HCP) solid solution structure [16, 17], so that the high-entropy alloy film can show the comprehensive performance of each component element [18]. High entropy alloys have four significant effects: thermodynamic high entropy effect, structural lattice distortion effect [19], kinetic hysteresis diffusion effect [20, 21], and characteristic cocktail effect [22, 23]. The lattice distortion effect makes it difficult for dislocations to occur within the alloy, thus improving the wear resistance of the alloy [24–26]. Meanwhile, the cocktail effect has been applied to the design of new wear-resistant alloys [27]. The previous study has shown that CoCrFeMnNiAl high entropy films form suboxide layers at high temperatures, and that the σ-phase formed in the subsurface oxide crystalline region contributes to the wear resistance of the film [28]. However, the mechanism of low friction due to high temperature oxidation of high entropy alloys is not entirely clear yet. And the structural characteristics of lubrication of high temperature oxidation products have not been revealed. These limit the development of high entropy alloy films in the field of high temperature lubrication.

In this work, it is proposed a strategy for *in-situ* forming lubricating phase on the surface of the designed VAlTiCrW high-entropy alloy film in order to obtain low friction coefficients at high temperatures. The oxide lubricating phase that determines the tribological properties and its formation inducement are analyzed in detail. The oxide products that determine the tribological performance of the films and its formation mechanism of oxidation and high-temperature tribochemistry are analyzed in detail. This provides a viable method for designing high-entropy alloy films with low friction property at elevated temperatures based on oxide lubrication.

2 Experiment

2.1 Principal elements design

The selection of metals was based on the two principles of high entropy alloy definition [24] and easy formation of Magnéli phase at high temperature [25], so five metals including vanadium, aluminum, titanium, chromium, and tungsten were selected. High entropy alloys require that these several elements have less difference radii and enable these elements to randomly occupy the lattice nodes to form disordered solid solutions. Meanwhile, both V and W have the potential to form Magnéli phases at high temperatures to endow high entropy alloy films with high-temperature lubricating characteristics. Aluminum can increase the hardness to improve the wear resistance of the film [29]. The larger atomic radius of titanium can increase the lattice distortion of the film and thus improve the hardness and strength, and is also beneficial to improve the wear resistance [30]. The addition of chromium can better improve the solid solubility of high entropy alloys [31].

2.2 Film preparation

VAlTiCrW high-entropy alloy films were deposited on superalloy substrate and silicon substrate by magnetron sputtering. The target comprises high-purity ($\geqslant$99.9%) vanadium, aluminum, titanium, chromium, and tungsten metal bars. To ensure the excellent adhesion of the film on the substrate surface, the superalloy substrate and silicon substrate are ultrasonically cleaned in acetone and ethanol for 20 minutes, respectively, and dried with nitrogen flow. Then the substrates are mounted on a rotatable holder and parallel to the target surface. To minimize the oxygen content in the film, the vacuum chamber is evacuated below 7.0×10^{-3} Pa before deposition.

The temperature inside the chamber is then maintained at 100 °C by temperature control module. The argon flow rate as the working gas is held at 30 sccm. At a bias voltage of 800 V, a duty cycle of 60%, and an ion beam voltage of 800 V, the substrate surface was etched for 30 minutes to remove impurities. At the end of etching, the ion beam is turned off, and then the film is deposited for 5 hours at the bias voltage of 400 V, the duty cycle of 60%, and the target current of 3 A.

2.3 Oxidation treatment

Atmospheric heat treatment of the VAlTiCrW films to achieve surface oxidation was carried out using a tube furnace. The heat treatment process was as follows: 700, 800, and 900 °C with a heating rate of 5 °C/min and a holding time of 1 h after reaching the set temperature. At the end of the holding time, it was cooled to room temperature in the furnace. The aim of the thermal treatment was to pre-form oxides on the surface of the films.

2.4 Microstructure characterization

The surface and cross-section of the coatings were observed using scanning electron microscope (SEM, American FEI company, Quanta FEG 250). And the content and distribution of elements in the films were determined by energy dispersive spectrometer (EDS). The crystal structure of the film was determined by X-ray diffractometer (XRD, German Bruker, D8 discover), the radiation uses Cu-Kα, the scattering angle range is 10°–100°, and the scanning speed is 5 (°)/min. The tribochemistry reaction product of the film was characterized using a Raman spectroscopy (British Renishaw company, invia reflex) with 532 nm band laser. Transmission electron microscopy (TEM, American ThemoFishe company, Talos F200x) was used to characterize the oxide scale, wear track, and transfer film on wear scar of its counterpart ball to analyze the tribological mechanism.

2.5 High-temperature friction test

The friction and wear properties of the films were measured using an high-temperature friction tester (Switzerland Anton Paar company, THT1000). The as-deposited film and pre-oxidized film were subjected to friction tests at 600, 700, and 800 °C with a frequency of 50 Hz, a load of 1 N, a radius of 5 mm, and a speed of 1 cm/s. Al_2O_3 ball with diameter of 6mm is selected as the counterpart ball. Al_2O_3 ball has high hardness (27.8 GPa) and high temperature stability [32]. And the total test time was 1,600 s.

The cross-sectional area of the wear tracks is measured using the surface profiler (American KLA-Tencor company, Alpha-Step IQ). Three measurements calculated the average wear rate at different locations of the wear tracks. The wear rate is calculated as follows:

$$\delta = \frac{\mathrm{V}}{\sum \mathrm{W}} = \frac{HA}{SF}$$

where δ is the wear rate in $mm^3/(N{\cdot}m)$, H is the total linear wear of the sample in mm, A is the cross-sectional area of the sample in mm^2, S is the total friction distance of the sample in m, and F is the load in N.

3 Results and discussion

3.1 Film composition and structure

The element content of the as-prepared VAlTiCrW film obtained by EDS is provided in Table 1, which is in the range of 5–35 at% defined by high-entropy alloy. The valence electron concentration VEC calculated from atomic percentage is 5.0332 according to the following formula:

$$\mathrm{VEC} = \sum_{i}^{n} c_i \mathrm{VEC}_i$$

where c_i is the atomic percentage of each element, and VEC_i is the valence electron concentration of each element.

It is generally believed that the BCC solid solution structure is more stable when the valence electron concentration VEC $\leqslant$ 6.87. In addition, V, Cr, and W elements are BCC structures, which makes the

Table 1 Element content in VAlTiCrW film.

VAlTiCrW film	V	Al	Ti	Cr	W
Composition (at%)	18.34	15.84	15.41	31.28	19.13

VAlTiCrW film easily form a BCC single solid solution structure. The XRD patterns show that the VAlTiCrW film has indeed a BCC structure (Fig. 1(a)). It is also noted that the film shows a wide BCC diffraction peak, indicating that a poor crystallinity. Figures 1(b) and 1(c) show the surface and cross-sectional morphologies of the as-prepared VAlTiCrW film with a thickness of about 4.6 μm. Although the VAlTiCrW film has a granular surface morphology and a columnar crystal cross section, the elements mapping shows that the VAlTiCrW film has a uniform element distribution. The selected area electron diffraction (SAED) pattern further shows that the VAlTiCrW film has a single-phase BCC polycrystalline structure (Fig. 1(d)).

3.2 Tribological properties of film

The friction coefficients of the as-prepared VAlTiCrW film at different temperatures as function of sliding time are shown in Fig. 2(a). The friction coefficient shows a downward trend with the elevated temperatures. At 600 °C, the VAlTiCrW film has a high friction coefficient of about 0.61. When the temperature rises to 700 °C, the friction coefficient stabilizes at about 0.43. When the temperature further reaches 800 °C, the friction coefficient is as low as about 0.15. The sudden jump of the friction coefficient may be caused by the local peeling and self-healing of the lubricating glaze layer. The great reduction of friction coefficient at 800 °C has aroused our interest. Therefore, the high-temperature friction experiments are carried out on the films pre-oxidized at different temperatures, as shown in Fig. 2(b). When the pre-oxidation temperature is the same as the friction experimental temperature, pre-oxidation has no effect on the friction coefficient of the film, which may be due to the similar oxidation products. Interestingly, the VAlTiCrW film pre-oxidized at 800 °C can obtain a very low friction coefficient of 0.2 at 700 °C, which is close to that of the as-prepared film at 800 °C. However, the friction coefficient of the pre-oxidized film at 600 °C returns to the high value similar to that of the as-prepared film at 600 °C, and even up to 0.71.

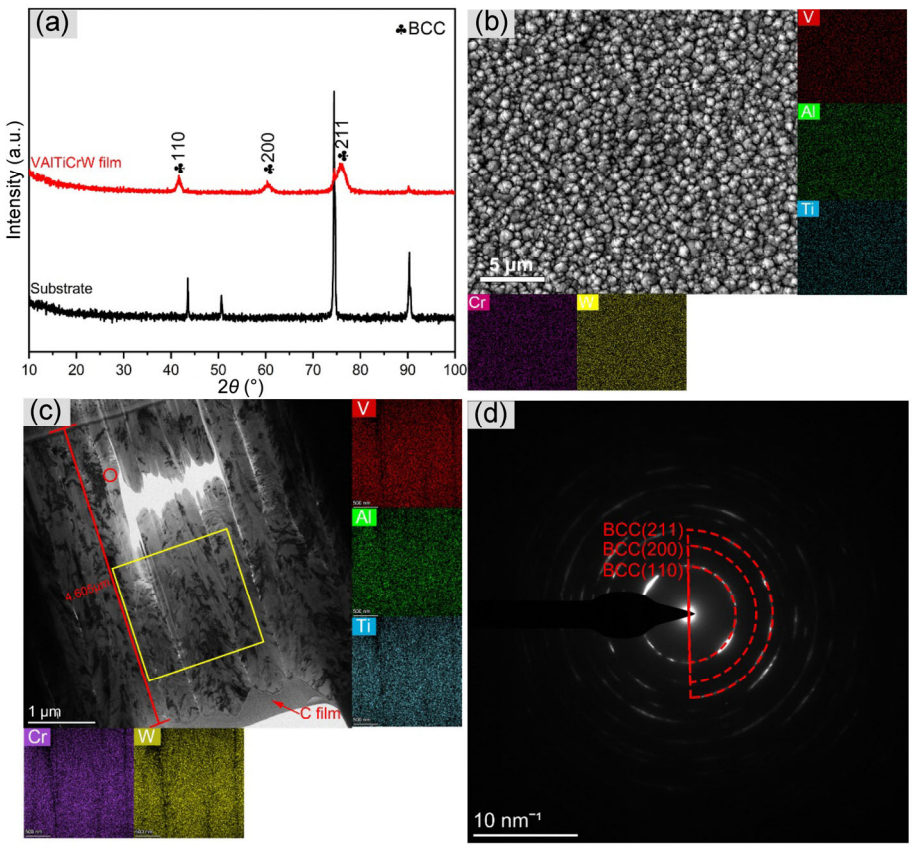

Fig. 1 XRD diffraction patterns (a), surface SEM image (b), and cross-sectional TEM image (c) of as-prepared VAlTiCrW film, SAED pattern in the red circle (d).

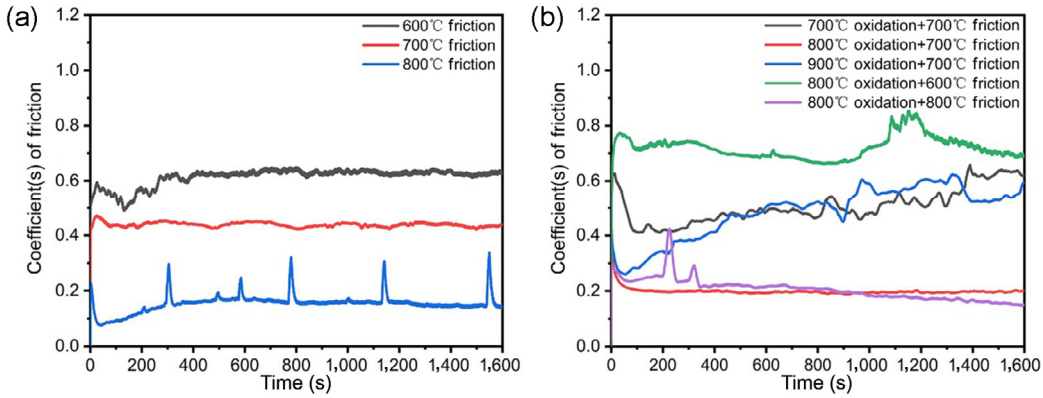

Fig. 2 Friction coefficient of VAlTiCrW films at different temperatures as a function of sliding time (a); friction coefficient of VAlTiCrW films pre-oxidized at different temperatures (b).

When the pre-oxidation temperature is further increased to 900 °C, unlike the film pre-oxidized at 800 °C, the friction coefficient of the film at 700 °C gradually increases until it is close to that of the as-prepared film at 700 °C. The special high-temperature friction phenomenon may be related to the oxidation products formed on the film surface. Therefore, the films subjected to heat-treatment and high-temperature friction are analyzed deeply below.

In order to understand the wear behavior of these films, SEM micrographs of wear tracks and calculated wear rates are shown in Fig. 3. The wear mechanism of the VAlTiCrW film at 600 °C is abrasive wear (Fig. 3(a)), and obvious grooves produced by abrasive particles appear on the wide wear track, which corresponds to its high friction coefficient. The wear track of the as-prepared film becomes narrow and smooth at 700 °C (Fig. 3(b)), with a very low wear rate of 1.97×10^{-5} $mm^3/(N\cdot m)$. However, when the ambient temperature further increased to 800 °C, although the as-prepared film had a lowest friction coefficient, its wear track becomes wider (Fig. 3(c)) and the wear rate increases slightly. This should be because the oxide lubricating phase with low melting point formed on the surface is easy to lose at higher temperature under the action of friction and extrusion, which can be reflected by the surface morphology of the high-temperature precipitates and obvious accretion of wear debris at the edge of wear track. The law of wear rate of the pre-oxidized films after friction test at different temperatures is similar to that of the as-prepared films, but increases significantly, except for this case that is the film pre-oxidized at 800 °C followed by friction at 600 °C. The wear morphology of this exceptional film is similar to that of the as-prepared film, but it is significantly narrower, which is reflected in a smaller wear rate. In addition, the wear rates of the VAlTiCrW films increase with the increase of pre oxidation temperature.

3.3 Analysis of friction mechanism

The oxide scale formed at high temperature plays an important role in friction. In order to discuss the effect of heat treatment on oxide layer, the morphologies and EDS mapping of the VAlTiCrW films oxidized at different temperatures were shown in Fig. 4. Compared with the as-prepared film (Fig. 1(b)), the surface morphology of the film changed little after oxidation at 700 °C (Fig. 4(a)). With the increase of oxidation temperature from 700 to 900 °C, the surface morphology of the film changes gradually. When the oxidation temperature is 800 °C, there are obvious penniform precipitates on the surface of the film (Fig. 4(b)). The element mapping image clearly shows that the precipitates are vanadium rich. At 900 °C, the granular structure on the surface of the film disappears due to element diffusion, but small pores are left (Fig. 4(c)). The element diffusion behavior at different temperatures can be better understood by the cross-sectional morphologies and EDS mapping of the films. The films have different degrees of oxidation at different temperatures. It can be seen from the mapping image that the contrast of surface oxygen element at 700 °C is higher than that of the cross section. Therefore, it is

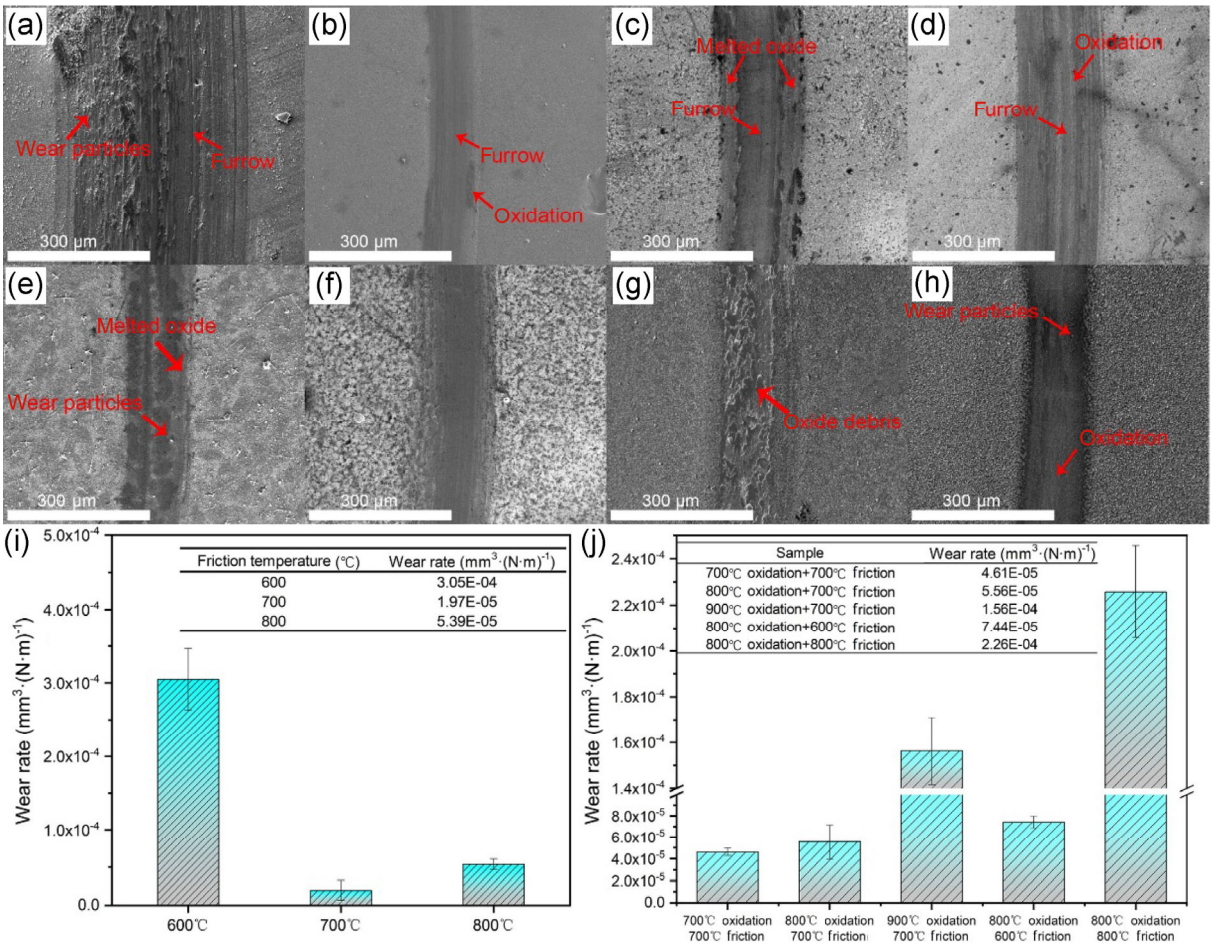

Fig. 3 SEM micrographs of wear tracks of the as-prepared films after friction at 600, 700, and 800 °C (a)–(c). Wear tracks of the films pre-oxidized at 700, 800, and 900 °C followed by friction at 700°C (d)–(f). Wear tracks of the films pre-oxidized at 800 °C followed by friction at 600 and 800 °C (g)–(h). Wear rate of the as-prepared films (i) and the pre-oxidized films (j).

judged that oxidation at 700 °C exists only in very thin areas on the surface. An identifiable oxide layer appears from 800 °C, and the thickness of the oxide layer increased with the increase of temperature, reaching roughly 1.1 μm at 800 °C and 1.7 μm at 900 °C. The element mapping image of the cross section shows that the elements in the films oxidized at 800 and 900 °C have obvious uphill diffusion, especially the Al elements. The V, Cr, and W elements enriched on the surface of the film after oxidation at 800 °C, while Ti diffuses heavily to the surface of the film after oxidation at 900 °C. It should be noted that the element segregation becomes more significant and Al enrichment layer gradually thickens with the increase of temperature. This composition evolution is conducive to the formation of high-temperature lubricating phase at 800 °C.

The VAlTiCrW films after oxidation and friction were characterized by XRD to study the oxide products corresponding to different tribological performance, as shown in Fig. 5. There are no distinct oxide peaks in the XRD spectra of the films rubbed at 600 °C and oxidized at 700 °C, but the peaks of $AlVO_4$, TiO_2, and Cr_2O_3 appear after friction at 700 °C (Fig. 5(a)). This should be because the film has formed a very thin oxide scale at the initial stage of 700 °C heat treatment, which prevents further oxidation. The oxide grains in the thin oxide scale are too small to be detected by XRD. However, the friction continuously destroys the oxide scale, which promotes the uphill diffusion of elements, oxidation reaction, and tribochemical reaction. The generated $AlVO_4$ ternary compound, which is mainly formed by Al^{3+} intercalation into V_2O_5 layer at high temperature, has high stability at high

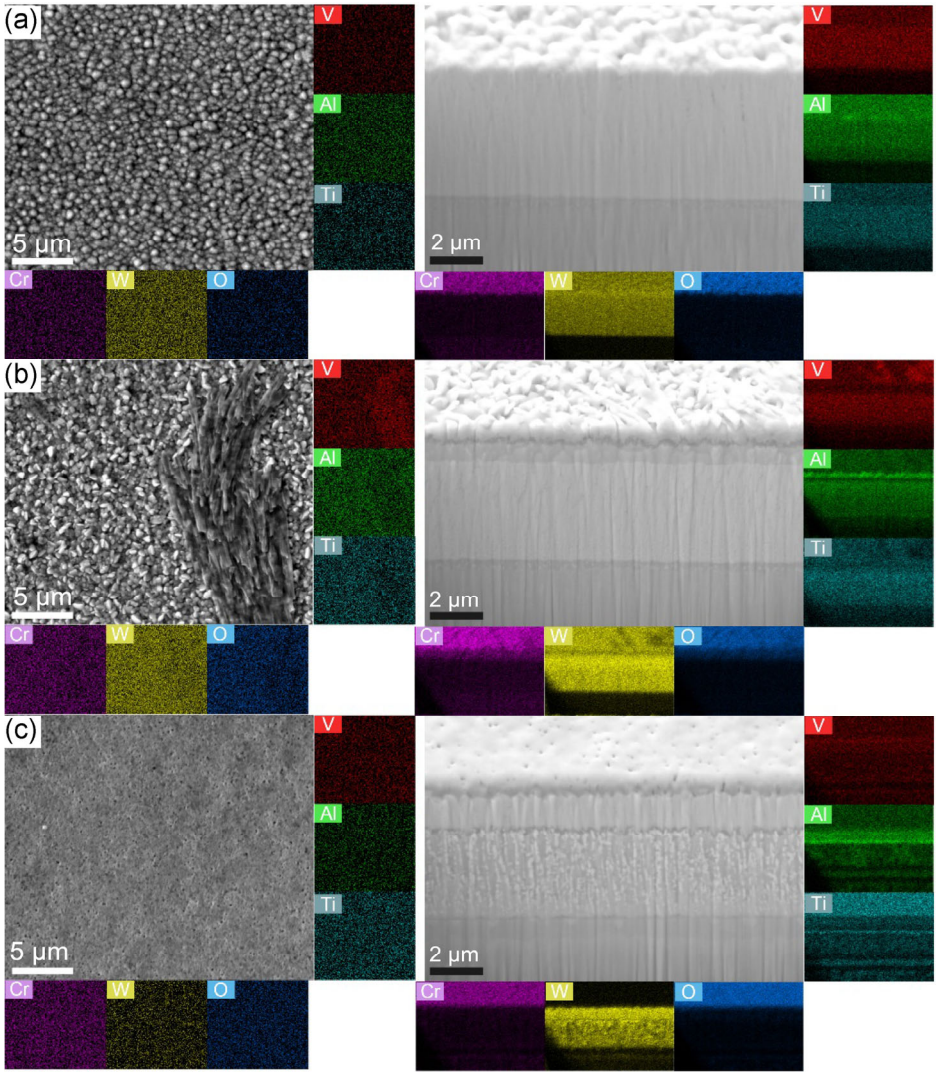

Fig. 4 SEM micrographs of surface and cross-sectional morphologies and EDS mapping images of the films after oxidation of 700 °C (a), 800 °C (b), and 900 °C (c)

temperature. $AlVO_4$, TiO_2, and Cr_2O_3 are abrasive phase at high temperature [33], resulting in relatively high friction coefficient of the as-prepared films at 700 °C. More oxide peaks appear in the XRD spectrum of the film rubbed at 800 °C (Fig. 5(a)). In addition to V_2O_5 peaks, there is a strong AlV_3O_9 peak at low angle. AlV_3O_9 is formed by the further reaction of $AlVO_4$ and V_2O_5 at high temperature [34–36], with large crystal plane spacing, which may be conducive to the realization of solid lubricity.

The XRD spectra of the samples after oxidation followed by friction show that the phase of the films oxidized at 800 °C followed by friction at 600 °C is not much different from that of the as-prepared films rubbed at 700 °C (Figs. 5(a) and 5(b)), and also has a high friction coefficient. However, when the oxidation is followed by friction at 700 °C, as the as-prepared film rubbed at 800 °C, there is a strong AlV_3O_9 diffraction peak at low angle (Fig. 5(b)), which can also achieve a very low friction coefficient. As for the films oxidized at 900 °C and the films oxidized at 900 °C followed by friction at 700 °C, the AlV_3O_9 peaks in the XRD spectra disappear and distinct Al_2O_3 peaks appear (Figs. 5(a) and 5(b)), which leads to the gradually increasing friction coefficient and high wear rate.

Therefore, it can be inferred that AlV_3O_9 can be formed spontaneously at 800 °C (Fig. 5(a)), but the main function of the special heat-treatment temperature should be to provide a precursor condition conducive

to the formation of AlV_3O_9, so that it can be generated in considerable amounts at 700 and 800 °C under the action of friction to obtain a lower friction coefficient. However, even though AlV_3O_9 has undergone oxidation at 800 °C, it cannot be formed under friction at 600 °C, because AlV_3O_9 will decompose into $AlVO_4$ and V_2O_5 at about 580 °C [37]. Moreover, AlV_3O_9 cannot exist stably at high temperature of 900 °C, perhaps as a result of the volatilization and decomposition of its precursor V_2O_5 at 900 °C (Fig. 5(a)), which ultimately fails to provide a formation condition of AlV_3O_9 in the friction experiment at 700 °C.

Raman analysis was carried out on the wear track of the film oxidized at 800 °C followed by 700 °C friction, and the film oxidized only at 800 °C, as shown in Fig. 6. The results show that the phases in the wear

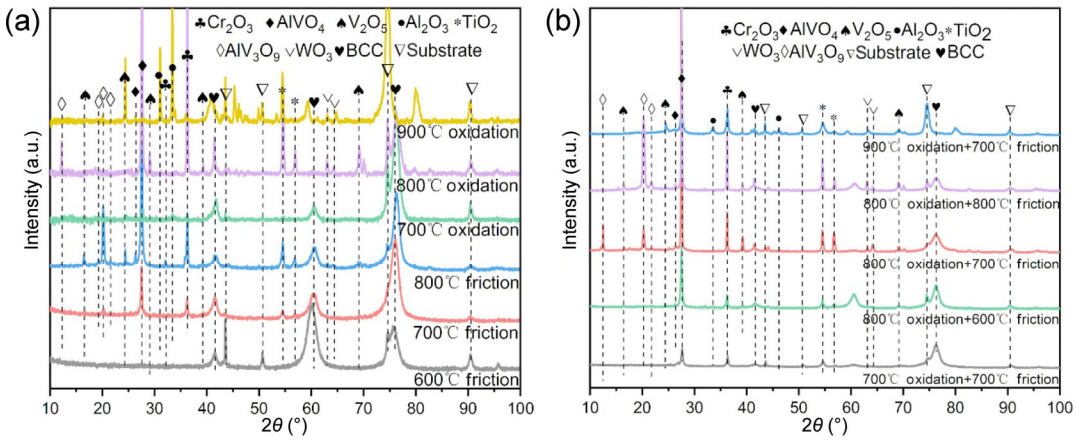

Fig. 5 XRD diffraction patterns of the film after oxidation or friction at different temperatures (a), and after oxidation followed rubbing at different temperatures (b).

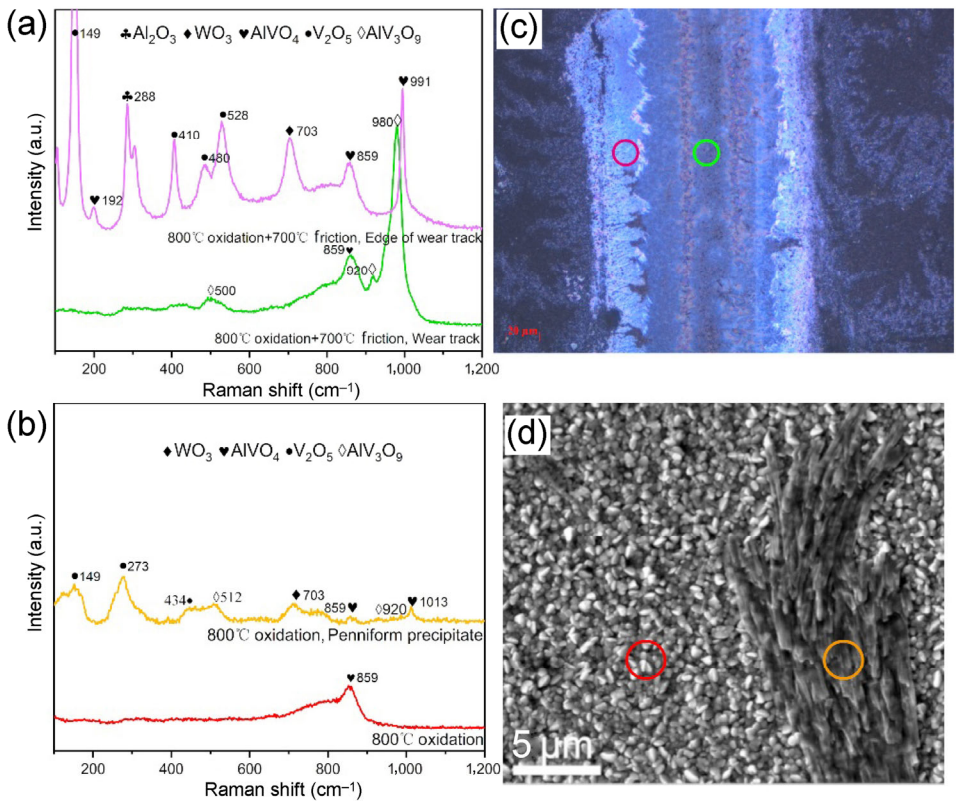

Fig. 6 Raman spectra of wear track of the film after oxidized at 800 °C followed by friction at 700 °C (a), and of the film after oxidation at 800 °C (b).

track and at the edge of the wear track are obviously different. The Raman peaks of Al_2O_3, WO_3, $AlVO_4$, and V_2O_5 appear at the edge of the wear track (Figs. 6(a) and 6(b)). The peaks at 149 and 410 cm^{-1} are the B_{1g} band vibration and V–O–V asymmetric stretching vibration of V_2O_5, and the strong peak at 991 cm^{-1} can be attributed to the V=O stretching vibration of $AlVO_4$ [35]. However, it is noted that the V=O peak in the wear track has an obvious red shift from 991 to 980 cm^{-1}, indicating that the V=O stretching vibration is weakened. The phenomenon of red shift is related to the structure when $AlVO_4$ changes to AlV_3O_9 [38], and the peak in the region of 512 cm^{-1} could be assigned to the (Al–O–V) asymmetric stretching vibration of AlV_3O_9. Therefore, it can be inferred that after oxidation at 800 °C, a large amount of vanadium precipitates to the surface and oxidizes to form V_2O_5, which is the main solid lubricating phase at the initial stage of 700 °C friction (Figs. 6(c) and 6(d)), although XRD results show that a small amount of AlV_3O_9 has been formed at 800 °C through solid-state reaction. Then, AlV_3O_9 was formed in considerable amounts through the tribochemical reaction of $AlVO_4$ and V_2O_5. In the meantime, since V_2O_5 with low melting point is pushed to the edge of the wear track under the action of friction, the solid lubricating phase in the wear track changes to AlV_3O_9 dominated.

In order to reveal the formation mechanism of AlV_3O_9 solid lubricating phase, TEM characterization was carried out for the film oxidized at 800 °C, and the wear track of the film with oxidation at 800 °C followed by friction at 700 °C, as shown in Fig. 7. After oxidation at 800 °C, an oxide scale with clear four layer is formed on the surface of the film (Fig. 7(a)), but the film under the oxide scale still maintains a columnar structure. Based on the analysis of element mapping and its content in different regions (Table 2), from the outside to the inside, there are about 100 nm V-rich layer dominated by V_2O_5 (feather precipitated phase region), large-grained oxide layer containing $AlVO_4$ phase, Al-rich layer dominated by Al_2O_3, and nanocrystalline layer with uniform oxide distribution. High-resolution TEM shows that $AlVO_4$ phase is formed at the junction of Al-rich oxide layer and V-rich oxide layer, which is produced by the solid-state reaction of elements at high temperature. The oxide layer on the wear track of the film rubbed at 700 °C

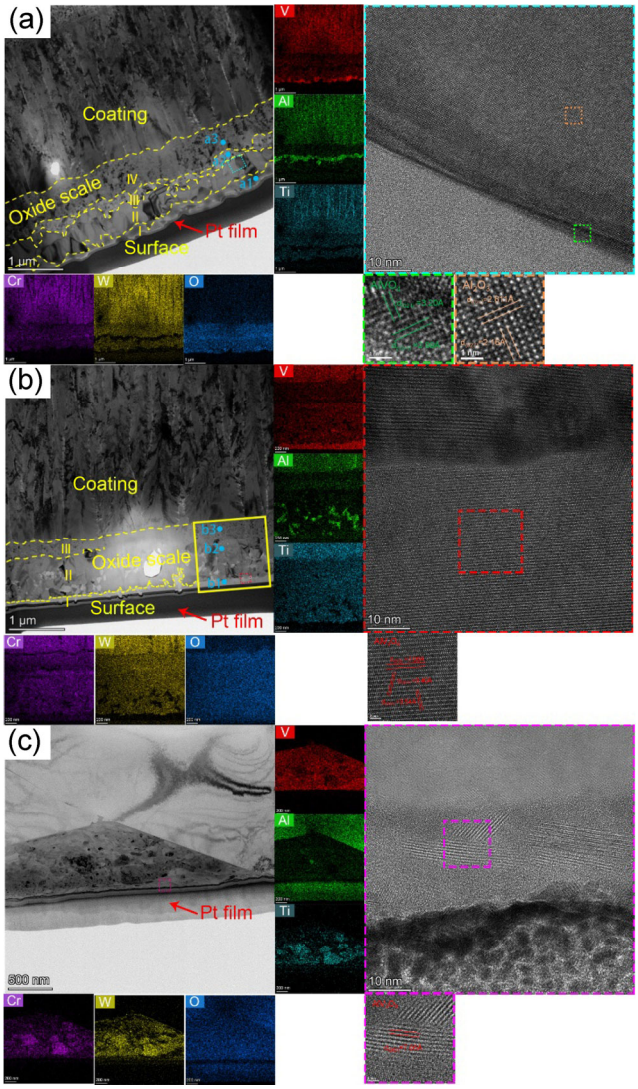

Fig. 7 Cross-sectional TEM images of the film after oxidation at 800 °C (a), wear track of the film after oxidation at 800 °C followed by friction at 700 °C (b), and transfer film on wear scar of its counterpart ball (c).

still has a multilayer structure (Fig. 7(b)), but the friction destroys the continuous Al_2O_3 layer, enabling Al_2O_3 and V_2O_5 to obtain sufficient contact, thus promoting the formation of a large number of $AlVO_4$ and AlV_3O_9 through tribochemical reaction. Further, its high-resolution TEM shows that the oxide in the outermost layer of the wear track is indeed AlV_3O_9 with preferred orientation of (002) crystal plane, and AlV_3O_9 also exists in transfer film on wear scar of its counterpart ball (Fig. 7(c)), which means that the stable antifriction substance of this friction system is indeed AlV_3O_9 formed under the thermal-mechanical action. However, so far, the research on the high-

Table 2 Atomic percentages of elements in different regions (at%) marked in Figs. 7(a) and 7(b).

Area	V	Al	Ti	Cr	W	O
a1	32.74	/	/	/	/	67.26
a2	5.75	25.12	/	4.92	/	64.21
a3	6.40	6.32	4.80	11.33	6.34	64.80
b1	26.97	5.94	0.4	6.75	0.7	59.25
b2	7.63	2.68	5.91	13.08	7.9	62.79
b3	4.63	3.27	5.21	12.26	8.39	66.25

temperature lubrication mechanism of AlV_3O_9 has not been reported. It is assumed that since the (002) crystal plane spacing of AlV_3O_9 is large, d = 0.7 nm, which makes the interlayer interaction force weak, so shear slip is easy to occur between layers. In addition, the high-temperature softening effect of AlV_3O_9 may also be the reason for the decrease of friction coefficient.

4 Conclusions

1) A uniform VAlTiCrW high-entropy alloy film with BCC structure was prepared by magnetron sputtering. The friction coefficient of this high-entropy alloy film continues to decrease with the increase of temperature from 600 to 800 °C, and drops to a very low value (0.15) at 800 °C, together with its good wear resistance.

2) A special friction phenomenon is that the film pre-oxidated at 800 °C can obtain a similar low friction coefficient of about 0.2 at 700 °C, but the higher oxidation temperature of 900 °C cannot achieve this low friction coefficient. It is found that the substance to achieve this low friction coefficient is a special ternary oxide AlV_3O_9, rather than the well-known high-temperature solid lubricating V_2O_5. A large number of V-rich oxides and Al-rich oxides through element diffusion, segregation, and oxidation at 800 °C, which can be fully contacted under the action of friction, are the prerequisite for the formation of AlV_3O_9. Thus, AlV_3O_9 is finally produced at 700 or 800 °C through the tribochemical reaction between Al_2O_3, $AlVO_4$, and V_2O_5, but lower or higher temperatures cannot.

3) This newly discovered high-temperature solid lubricating material has a very large (002) crystal plane spacing. The formed preferentially oriented crystal surface may make the VAlTiCrW film obtain a very low friction coefficient at high temperature through interlayer slippage. Of course, high-temperature softening may also be another reason. This study will help to explore new high-temperature solid lubricating substances and mechanisms.

Acknowledgements

The work was supported by the National Key R&D Program of China (No. 2018YFB2000300), the Zhejiang Provincial Natural Science Foundation (No. LR20E050001), the National Science and the Technology Major Project (No. 2017-VII-0013-0110), and National Natural Science Foundation of China (No. 51775539).

References

[1] Aouadi S M, Gao H, Martini A, Scharf T W, Muratore C. Lubricious oxide coatings for extreme temperature applications: A review. *Surf Coat Technol* **257**: 266–277 (2014)

[2] Zhu S Y, Cheng J, Qiao Z H, Yang J. High temperature solid-lubricating materials: A review. *Tribol Int* **133**: 206–223 (2019)

[3] Wan S H, Tieu A K, Xia Y N, Zhu H T, Tran B H, Cui S G. An overview of inorganic polymer as potential lubricant additive for high temperature tribology. *Tribol Int* **102**: 620–635 (2016)

[4] Wang W Z, Zheng S X, Pu J B, Cai Z B, Wang H X, Wang L P, He G Y. Microstructure, mechanical and tribological properties of Mo-V-N films by reactive magnetron sputtering. *Surf Coat Technol* **387**: 125532 (2020)

[5] Rathaur A S, Katiyar J K, Patel V K. Thermo-mechanical and tribological properties of SU-8/h-BN composite with SN150/perfluoropolyether filler. *Friction* **8**(1): 151–163 (2020)

[6] Scharf T W, Prasad S V. Solid lubricants: A review. *J Mater Sci* **48**(2): 511–531 (2013)

[7] Meng Y G, Xu J, Jin Z M, Prakash B, Hu Y Z. A review of recent advances in tribology. *Friction* **8**(2): 221–300 (2020)

[8] Zabinski J S, Donley M S, Dyhouse V J, McDevitt N T. Chemical and tribological characterization of PbO–MoS_2 films grown by pulsed laser deposition. *Thin Solid Films* **214**(2): 156–163 (1992)

[9] Xu Z, Zhang Q, Zhai W. Tribological properties of TiAl matrix self-lubricating composites incorporated with tungsten disulfide and zinc oxide. *RSC Adv* **5**(56): 45044–45052 (2015)

[10] Liu E Y, Bai Y P, Gao Y M, Yi G W, Jia J H. Tribological properties of NiAl-based composites containing Ag_3VO_4 nanoparticles at elevated temperatures. *Tribol Int* **80**: 25–33 (2014)

[11] Feng X C, Lu C, Jia J H, Xue J L, Wang Q H, Sun Y, Wang W Z, Yi G W. High temperature tribological behaviors and wear mechanisms of NiAl-NbC-Ag composites formed by *in situ* decomposition of $AgNbO_3$. *Tribol Int* **141**: 105898 (2020)

[12] Stott F H, Wood G C. The influence of oxides on the friction and wear of alloys. *Tribol Int* **11**(4): 211–218 (1978)

[13] Erdemir A. A crystal chemical approach to the formulation of self-lubricating nanocomposite coatings. *Surf Coat Technol* **200**(5–6): 1792–1796 (2005)

[14] Magnéli A. Structures of the ReO_3-type with recurrent dislocations of atoms: `homologous series' of molybdenum and tungsten oxides. *Acta Cryst* **6**(6): 495–500 (1953)

[15] Zhao Y Q, Mu Y T, Liu M. Mechanical properties and friction–wear characteristics of VN/Ag multilayer coatings with heterogeneous and transition interfaces. *Trans Nonferrous Met Soc China* **30**(2): 472–483 (2020)

[16] Huang T D, Jiang H, Lu Y P, Wang T M, Li T J. Effect of Sc and Y addition on the microstructure and properties of HCP-structured high-entropy alloys. *Appl Phys A* **125**(3): 180 (2019)

[17] Guo S, Ng C, Lu J, Liu C T. Effect of valence electron concentration on stability of fcc or bcc phase in high entropy alloys. *J Appl Phys* **109**(10): 103505 (2011)

[18] Guo S, LIU C T. Phase stability in high entropy alloys: Formation of solid-solution phase or amorphous phase. *Prog Nat Sci Mater Int* **21**(6): 433–446 (2011)

[19] Yeh J W, Chang S Y, Hong Y D, Chen S K, Lin S J. Anomalous decrease in X-ray diffraction intensities of Cu-Ni-Al-Co-Cr-Fe-Si alloy systems with multi-principal elements. *Mater Chem Phys* **103**(1): 41–46 (2007)

[20] Yeh J W. Recent progress in high-entropy alloys. *Ann Chim Sci Mat* **31**(6): 633–648 (2006)

[21] Tsai K Y, Tsai M H, Yeh J W. Sluggish diffusion in Co-Cr-Fe-Mn-Ni high-entropy alloys. *Acta Mater* **61**(13): 4887–4897 (2013)

[22] Kao Y F, Chen T J, Chen S K, Yeh J W. Microstructure and mechanical property of as-cast, -homogenized, and -deformed Al_xCoCrFeNi ($0 \leqslant x \leqslant 2$) high-entropy alloys. *J Alloys Compd* **488**(1): 57–64 (2009)

[23] Zhang Y, Zuo T T, Tang Z, Gao M C, Dahmen K A, Liaw P K, Lu Z P. Microstructures and properties of high-entropy alloys. *Prog Mater Sci* **61**: 1–93 (2014)

[24] Alvi S, Jarzabek D M, Kohan M G, Hedman D, Jenczyk P, Natile M M, Vomiero A, Akhtar F. Synthesis and mechanical characterization of a CuMoTaWV high-entropy film by magnetron sputtering. *ACS Appl Mater Interfaces* **12**(18): 21070–21079 (2020)

[25] Joseph J, Stanford N, Hodgson P, Fabijanic D M. Understanding the mechanical behaviour and the large strength/ductility differences between FCC and BCC Al_xCoCrFeNi high entropy alloys. *J Alloys Compd* **726**: 885–895 (2017)

[26] Joseph J, Haghdadi N, Shamlaye K, Hodgson P, Barnett M, Fabijanic D. The sliding wear behaviour of CoCrFeMnNi and Al_xCoCrFeNi high entropy alloys at elevated temperatures. *Wear* **428–429**: 32–44 (2019)

[27] Cui Y, Shen J Q, Manladan S M, Geng K P, Hu S S. Wear resistance of FeCoCrNiMnAl_x high-entropy alloy coatings at high temperature. *Appl Surf Sci* **512**: 145736 (2020)

[28] Joseph J, Haghdadi N, Shamlaye K, Hodgson P, Barnett M, Fabijanic D. The sliding wear behaviour of CoCrFeMnNi and Al_xCoCrFeNi high entropy alloys at elevated temperatures. *Wear* **428–429**: 32–44 (2019)

[29] Cheng H, Fang Y H, Xu J M, Zhu C D, Dai P Q, Xue S X. Tribological properties of nano/ultrafine-grained FeCoCrNiMnAl_x high-entropy alloys over a wide range of temperatures. *J Alloys Compd* **817**: 153305 (2020)

[30] Hsu Y C, Li C L, Hsueh C H. Modifications of microstructures and mechanical properties of CoCrFeMnNi high entropy alloy films by adding Ti element. *Surf Coat Technol* **399**: 126149 (2020)

[31] Zhang M D, Zhang L J, Fan J T, Li G, Liaw P K, Liu R P. Microstructure and enhanced mechanical behavior of the $Al_7Co_{24}Cr_{21}Fe_{24}Ni_{24}$ high-entropy alloy system by tuning the Cr content. *Mater Sci Eng A* **733**: 299–306 (2018)

[32] Deng W, Tang L, Zhang C F, Qi H. Tribological behaviours of 8YSZ coating sliding against different counterparts. *Surf Eng* **37**(1): 111–119 (2021)

[33] Kutschej K, Mayrhofer P H, Kathrein M, Polcik P, Mitterer C. Influence of oxide phase formation on the tribological behaviour of Ti-Al-V-N coatings. *Surf Coat Technol* **200**(5–6): 1731–1737 (2005)

[34] Steinfeldt N, Müller D, Berndt H. VO_x species on alumina at high vanadia loadings and calcination temperature and their role in the ODP reaction. *Appl Catal A Gen* **272**(1–2): 201–213 (2004)

[35] Brázdová V, Ganduglia-Pirovano M V, Sauer J. Crystal structure and vibrational spectra of AlVO4. A DFT study. *J Phys Chem B* **109**(1): 394–400 (2005)

[36] Shah P R, Khader M M, Vohs J M, Gorte R J. A comparison of the redox properties of vanadia-based mixed oxides. *J Phys Chem C* **112**(7): 2613–2617 (2008)

[37] Deramond E, Savariault J M. Aluminium oxide intercalation in vanadium oxibronzes via soft chemistry. *Mater Res Bull* **28**(8): 749–755 (1993)

[38] Low W H, Lim S S, Chia C H, Siong C W, Khiew P S. Three-dimensional lion's mane like AlV_3O_9 deposited on graphene surface for supercapacitors with a promising electrochemical performance. *J Sci Adv Mater Devices* **5**(2): 164–172 (2020)

Xuesong LIU. He received his bachelor degree in light chemical engineering in 2018 from Nanjing Tech University, Nanjing, China. From 2019 to 2022, he studied for a master degree in chemical engineering at Guangxi University, Guangxi, China. From 2020 to 2022, as a joint cultivations' master degree students, he took part in research work in Ningbo Institute of Material Technology and Engineering, Chinese Academy of Sciences, Ningbo, China. His research interests are high temperature tribological properties of high entropy alloy coatings.

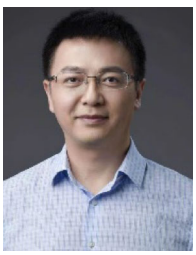

Jibin PU. He received his Ph.D. degree in 2012 from Lanzhou Institute of Chemical Physics, Chinese Academy of Sciences, Lanzhou, China. From 2012 to 2015, he carried out research work in Lanzhou Institute of Chemical Physics, Chinese Academy of Sciences, Lanzhou, China. Then, he joined the Ningbo Institute of Materials Technology and Engineering, Chinese Academy of Sciences, Ningbo, China. His current position is a professor. His research areas focus on coating design and tribology science in extreme environments. So far, he has published over 100 SCI papers.

Zhaoxia LU. She received the M.S. and Ph.D. degrees in chemical technology from Guangxi University, China, in 2006 and 2021, respectively, and her bachelor degree in chemical equipment and machinery in 1993 from Guangxi University, China. She joined the College of Chemistry and Chemical Engineering at Guangxi University from 1993. Her current position is an associate professor. Her research areas focus on the corrosion science and tribology of metal.